Phonon-Dressed Mollow Triplet in the Regime of Cavity Quantum Electrodynamics: Excitation-Induced Dephasing and Nonperturbative Cavity Feeding Effects

C. Roy and S. Hughes*

Department of Physics, Queen's University, Kingston, Ontario K7L 3N6, Canada

(Received 1 February 2011; revised manuscript received 13 March 2011; published 16 June 2011)

We study the resonance fluorescence spectra of a driven quantum dot placed inside a high-Q semiconductor cavity and interacting with an acoustic phonon bath. The dynamics is calculated using a time-convolutionless master equation in the polaron frame. We predict pronounced spectral broadening of the Mollow sidebands through off-resonant cavity emission which, for small cavity-coupling rates, increases quadratically with the Rabi frequency in direct agreement with recent experiments using semiconductor micropillars [S. M. Ulrich *et al.*, preceding Letter, Phys. Rev. Lett. **106**, 247402 (2011)]. We also demonstrate that, surprisingly, phonon coupling actually helps resolve signatures of the elusive second rungs of the Jaynes-Cummings ladder states via off-resonant cavity feeding. Both multiphonon and multiphoton effects are shown to play a qualitatively important role on the fluorescence spectra.

DOI: 10.1103/PhysRevLett.106.247403 PACS numbers: 78.67.Hc, 42.50.Ct, 78.55.−m

Recent developments in semiconductor cavity systems combine several fields of research, including semiconductor optics, quantum information processing and cavity QED (quantum electrodynamics). Target quantum sources such as indistinguishable photons are important in technological applications [1], and require robust physics designs and an understanding of how to manipulate dynamical processes at a very fundamental level. Unique quantum processes can be obtained when the cavity and quantum dot (QD) are near the strong coupling regime [2,3], which introduces quantum mechanical features such as photon antibunching [4]. Experimental studies involving coherent excitation have focussed on resonance fluorescence of a QD coupled to a cavity mode [5–7]. Also of interest is the study of off-resonant QD cavity systems that can be used to monitor resonance fluorescence of the emitter [8]. Large optical dipole moments relative to atomic systems and strong interaction effects are the salient features of these QDs.

In 1969, Mollow demonstrated that the fluorescence spectrum of a two-level atom, which represents the intensity of the incoherently scattered light, has additional sidebands in addition to the central coherent peak when the atom is driven by a strong coherent single-mode field [9,10]. This effect can be attributed to the emergence of "dressed states"—an infinite series of doublets or Floquet states, whose positions and spectral widths can be probed by experimentally measuring the spectrally resolved emission intensity. It is of fundamental interest to study such well-known atomic optics effects when a semiconductor QD is strongly driven by a coherent laser field. For pulsed-excited systems, excitation-induced dephasing (EID) emerges due to the interaction of the laser-induced dressed states with the underlying acoustic phonon reservoir [11–13]. For continuous wave (cw) excitation, it is not clear what the role of phonon coupling will be, as it is often argued that the dephasing processes are especially important for short pulses and fast time scales. Thus one may expect that cw excitation does not suffer much from phonon-induced damping, and indeed experimental measurements of the QD resonance fluorescence [5–7] suggest negligible influence from the phonon bath. Nevertheless, if a QD system is driven strongly enough, a phonon-induced dephasing process may occur [14]. In recent experiments [15], cw resonance fluorescence emission from a single QD placed inside a high-quality micropillar cavity was studied. In contrast to previous works on cw-excited semiconductor systems, it was found that increasing excitation power results in a Mollow triplet spectrum with a systematic spectral sideband broadening that is proportional to the square of the Rabi frequency—which was interpreted as a signature of EID [11,12]. Since the QD was placed in the regime of cavity QED, which enables significant cavity coupling, the origin of this Mollow sideband dephasing is not at all clear. To the best of our knowledge there has been no theoretical work dealing with such a fascinating excitation regime.

In this Letter, we develop a time-convolutionless master equation (ME) model that describes electron-acoustic phonon coupling and cavity photon coupling to all orders. Specifically, we describe the process of electron-longitudinal acoustic (LA) phonon coupling by using a polaron transform [16], and include electron-photon coupling, nonperturbatively; the resulting ME, in the appropriate limits, formally recovers the independent boson model or the Jaynes-Cumming model. A similar model was introduced by Wilson-Rae and Imamoglǔ using a more complex ME, which was solved in the linear excitation domain. The polaron transform allows one to eliminate the QD phonon interaction part from the system Hamiltonian at the expense of modified Rabi frequency, and the dot-cavity coupling that is now dressed by coherent phonon displacement operators [16,17]. We apply this theory to introduce new regimes of phonon-dressed semiconductor cavity QED, and we make a direct connection to the recent observations of EID on the semiconductor Mollow triplet [15].

Defining η_x as the coherent pump rate of the exciton, and working in a frame rotating with respect to the laser pump frequency, ω_L, the model Hamiltonian is

$$H = \hbar\Delta_{xL}\sigma^+\sigma^- + \hbar\Delta_{cL}a^\dagger a + \hbar g(\sigma^+ a + a^\dagger\sigma^-) + \hbar\eta_x(\sigma^+ + \sigma^-) + \sigma^+\sigma^-\sum_q \hbar\lambda_q(b_q + b_q^\dagger) + \sum_q \hbar\omega_q b_q^\dagger b_q, \quad (1)$$

where $b_q(b_q^\dagger)$ are the annihilation and creation operators of the phonon reservoir, a is the leaky cavity-mode annihilation operator, σ^+, σ^- (and $\sigma^z = \sigma^+\sigma^- - \sigma^-\sigma^+$) are the Pauli operators of the electron-hole pair (''exciton''), $\Delta_{\alpha L} \equiv \omega_\alpha - \omega_L$ ($\alpha = x, c$) are the detunings of the exciton and cavity from the coherent pump laser, λ_q is the exciton-phonon interaction, and g is the cavity-exciton coupling strength. Performing a polaron-transformation introduces a renormalized Rabi frequency and dot-cavity coupling strength [17]: $H' = \exp(S)H\exp(-S)$, with $S = \sigma^+\sigma^-\sum_q \frac{\lambda_q}{\omega_q}(b_q^\dagger - b_q)$. The transformed Hamiltonian has three contributions,

$$H'_{\rm sys} = \hbar(\Delta_{xL} - \Delta_P)\sigma^+\sigma^- + \hbar\delta_{cL}a^\dagger a + \langle B\rangle X_g, \quad (2)$$

$$H'_{\rm bath} = \sum_q \hbar\omega_q b_q^\dagger b_q, \qquad H'_{\rm int} = X_g\zeta_g + X_u\zeta_u, \quad (3)$$

where $X_g = \hbar g(a^\dagger\sigma^- + \sigma^+ a) + \hbar\eta_x(\sigma^+ + \sigma^-)$, $X_u = i\hbar[g(\sigma^+ a - a^\dagger\sigma^-) + \eta_x(\sigma^- - \sigma^+)]$, $B_\pm = \exp[\pm\sum_q \frac{\lambda_q}{\omega_q}\times(b_q - b_q^\dagger)]$, $\zeta_g = \frac{1}{2}(B_+ + B_- - 2\langle B\rangle)$, and $\zeta_u = \frac{1}{2i}\times(B_+ - B_-)$. Note that $\langle B\rangle = \langle B_+\rangle = \langle B_-\rangle$ and the polaron shift is given by $\Delta_P = \sum_q \frac{\lambda_q^2}{\omega_q}$. Without loss of generality, we assume that the polaron shift is implicitly included in ω_x. For the QDs of interest, the interaction between the system and phonon bath can be characterized by the spectral function [17–19] $J(\omega) = \sum_q |\lambda_q|^2\delta(\omega - \omega_q)$. It is important to note the slightly different definition of the system Hamiltonian in Eq. (2). The usual decomposition of the system Hamiltonian to include only the noninteracting QD and cavity parts is known to fail the detailed balance condition in general, which is caused by internal coupling [20]. The transformed system Hamiltonian above leads to the correct form of the density operator and preserves detailed balance. A previous example of internal coupling on the phonon-modified vacuum Rabi splitting yields an *asymmetric* doublet [17,19,21,22].

Next, we introduce phenomenological dissipative terms that describe the radiative decay of the QD exciton and the cavity mode. They are included as Liouvillian superoperators [19]: $L(\rho) = \frac{\tilde{\Gamma}_x}{2}(2\sigma^-\rho\sigma^+ - \sigma^+\sigma^-\rho - \rho\sigma^+\sigma^-) + \kappa(2a\rho a^\dagger - a^\dagger a\rho - \rho a^\dagger a) + \frac{\Gamma'}{4}(\sigma_z\rho\sigma_z - \rho)$, where 2κ is the cavity decay rate, Γ' is the pure dephasing rate, and $\tilde{\Gamma}_x = \Gamma_x\langle B\rangle^2$ with Γ_x the bare radiative decay rate. The latter decay has an additional renormalization by a factor of $\langle B\rangle^2$ due to the dephasing of the optical dipole moment resulting from the Franck-Condon displacement of the excited state [23]. Since time scales associated with phonons are very fast compared to radiative processes, the coherent phonon displacement operators $B_\pm$ can be replaced by $\langle B\rangle = \langle B_\pm\rangle$.

We now derive a time-local ME [18] using the time-convolutionless approach for the cavity-QED system density operator in the interaction picture, described by $H'_{\rm sys}$, and to second order in exciton-photon-phonon coupling $H'_{\rm int}$—which describes the phonon-induced scattering between the cavity-coupling and laser-induced dressed states of the CQED system; this latter second-order phonon-induced scattering term is then treated within a standard bath approximation. The phonon reservoir is also considered to be stationary and in thermal equilibrium and factorized initial conditions are assumed. The time-convolutionless ME for the cavity-QED system density operator is then given by

$$\frac{\partial\rho}{\partial t} = \frac{1}{i\hbar}[H'_{\rm sys}, \rho(t)] + L(\rho) - \frac{1}{\hbar^2}\int_0^t d\tau \sum_{m=g,u} \times (G_m(\tau)[X_m, e^{-iH'_{\rm sys}\tau/\hbar}X_m e^{iH'_{\rm sys}\tau/\hbar}\rho(t)] + \text{H.c.}), \quad (4)$$

where $G_{g/u}(t) = \langle\zeta_{g/u}(t)\zeta_{g/u}(0)\rangle$. These polaron Green functions are well known and are defined as [16,17] $G_g(t) = \langle B\rangle^2(\cosh[\phi(t)] - 1)$, $G_u(t) = \langle B\rangle^2\sinh[\phi(t)]$, with $\phi(t) = \int_0^\infty d\omega\frac{J(\omega)}{\omega^2}[\coth(\beta\hbar\omega/2)\cos(\omega t) - i\sin(\omega t)]$. The $\langle B\rangle$ and the polaron shift Δ_P depend on the phonon spectral function through $\langle B\rangle = \exp[-\frac{1}{2}\int_0^\infty d\omega\frac{J(\omega)}{\omega^2}\times\coth(\beta\hbar\omega/2)]$ and $\Delta_P = \int_0^\infty d\omega\frac{J(\omega)}{\omega}$. This model describes the electron-LA-phonon interaction via a deformation potential coupling which is the primary source of dephasing in self-assembled QDs [24]. The spectral function that considers electron-phonon interactions via a deformation potential coupling can now be written as $J(\omega) = \alpha_p\omega^3\exp(-\omega^2/2\omega_b^2)$ where we use $\omega_b = 1$ meV and $\alpha_p/(2\pi)^2 = 0.06$ ps^2 as typical numbers for InAs/GaAs QDs [22,25]. With these parameters, the phonon-induced renormalization of the coherent drive and g, e.g., at $T = 10$ K is $\langle B\rangle = 0.84$. With the polaron ME, we can readily calculate the cavity-mode incoherent spectrum, $S_{\rm cav}(\omega) \propto \lim_{t\to\infty}\text{Re}\{\int_0^\infty d\tau[\langle a^\dagger(t+\tau)a(t)\rangle - \langle a^\dagger(t+\tau)\rangle\langle a(t)\rangle]e^{i(\omega_L-\omega)\tau}\}$. The ME is numerically solved in a basis that can be truncated at any arbitrary photon and exciton state, which enables us to compute the weak excitation approximation results (one-photon limit) and the regime of multiphoton cavity QED. The two-time correlation function is obtained from the quantum regression formula [10]. Since we consider cw excitation, and the phonon dephasing time scales are very fast, we can take $t \to \infty$ in the integral of Eq. (4); we have checked this

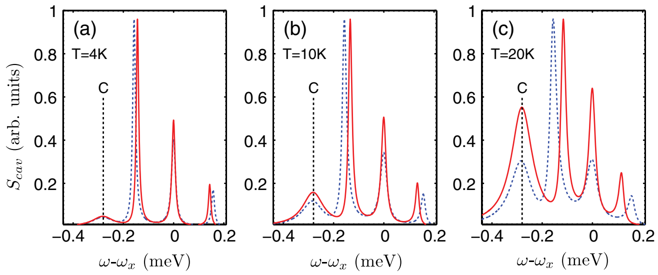

FIG. 1 (color online). Cavity-emitted fluorescence spectra for the one-phonon model (blue dashed line) and the full polaron theory (red solid line), for various temperatures. Photons are included to all orders [cf. Figure 2]. The cw Rabi drive strength $\eta_x = 80\ \mu$eV, and is resonant with the exciton ($\Delta_{xL} = 0$). The parameters are as follows: $g = 50\ \mu$eV, $\Gamma' = 2\ \mu$eV, $\tilde{\Gamma}_x = 1\ \mu$eV, $2\kappa = 0.1$ meV and $\omega_x - \omega_c = 0.28$ meV.

approximation to be rigorously valid. Thus any driving dependence of the field is through sampling the spectral bath at different frequencies, and not related to non-Markovian effects—all terms in our ME are local in time.

We first assess the role of both multiphonons and multiphotons. To be consistent with the recent Mollow triplet experiments on semiconductor micropillars [15], we consider a detuned cavity mode with $\omega_x - \omega_c = 0.28$ meV (unless stated otherwise), a cw resonantly excited exciton, and $g = 50\ \mu$eV. The radiative decay rate $\tilde{\Gamma}_x = 1\ \mu$eV and the residual pure dephasing rate, $\Gamma' = 2\ \mu$eV; these are similar to those obtained by Ulrich *et al.* [15], and between those measured in Refs. [1,6]. In Fig. 1, we plot the cavity-emitted spectrum for the one-phonon model and compare it with the full polaron theory. The one-phonon correlation function is obtained by expanding the phonon correlation functions $G_{g,u}(t)$, and $\langle B \rangle$, to lowest order in the dot-phonon coupling. At low temperatures, the one-phonon expansion of the polaronic phonon correlation function is sufficient to describe the dynamics. However, with increasing temperatures, the one-phonon model starts to deviate from the polaronic description; this trend is consistent with the pulse-excitation analysis of McCutcheon and Nazir [18], for $T > 30$ K (with no cavity). What is particularly surprising in our present case is that multiphonon effects are important already at $T = 10$ K and significant at $T \geq 20$ K (these trends become more pronounced as g and η_x are increased); notably, the cavity peak and the FWHM of the central peak of the Mollow triplet are underestimated by about 50%. For clarity we have assumed a fixed Γ' though this will also increase as a function of temperature.

In Fig. 2 we study the role of multiphoton processes in the QD cavity emission in the presence of phonons, again for $g = 50\ \mu$eV; Fig. 2(a) has no phonon coupling, while Figs. 2(b) and 2(c) include phonon coupling—with the cavity detuned by $\omega_x - \omega_c = \pm 0.28$ meV. We identify two remarkable features in the cavity-emitted spectrum. First, there is a strong asymmetry for the on-resonance Mollow triplet, which is due to the off-resonant cavity and

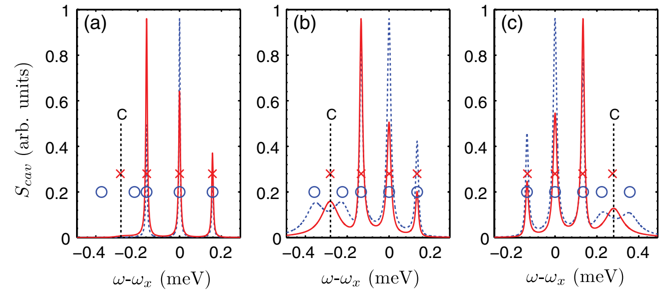

FIG. 2 (color online). Cavity-emitted fluorescence spectra with multiphoton processes (red solid line) compared to one-photon processes (blue dashed line), at $T = 10$ K. In (a) we have phonons off (apart from pure dephasing), while in (b) and (c), we consider phonon interactions with the cavity on either side of the exciton ($\omega_x - \omega_c = \pm 0.28$ meV). Here we consider phonons to all orders, with parameters as in Fig. 1. We also plot the dominant dressed-state resonance transitions associated with one-photon (blue circles) and two-photon truncations (red crosses) of the ME (see text).

phonon coupling. Second, there is a pronounced cavity feeding effect, where the cavity mode is excited via phonon interactions, which is a similar phenomenon to what happens for incoherently excited QD-cavity systems [19,22,25,26]. When the cavity is redshifted from the exciton, a more pronounced cavity coupling is obtained as the exciton decay excites the cavity mode via phonon emission, an effect which is also influenced by the cw drive. By inspecting the phonon contributions in the ME, we find "quantum jump" terms that scale with g^2, $\eta_x g$, and η_x^2. We also clearly see that a one-photon-correlation approximation fails, though a two-photon-correlation basis was found to be sufficient for all the calculations that follow. We further calculate the dressed-state eigenvalues (quasienergy eigenvalues) associated with the one-photon and

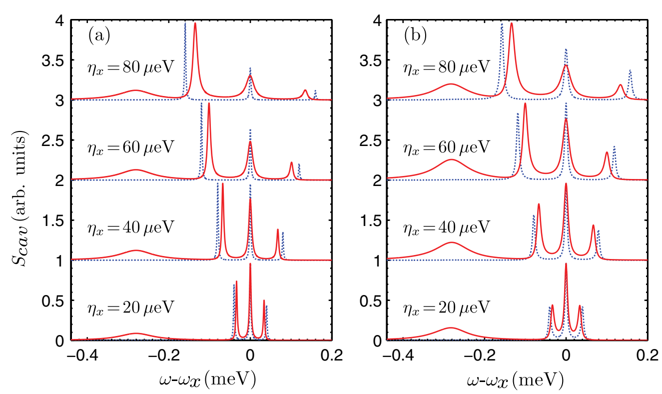

FIG. 3 (color online). Cavity-emitted fluorescence spectra of a QD placed under cw excitation of the exciton. We vary the Rabi frequency η_x from 20–80 μeV, and consider two different QD-cavity couplings: (a) $g = 15\ \mu$eV and (b) $g = 50\ \mu$eV. The blue dashed plots correspond to the cases with no phonon-coupling, while the red solid line corresponds to the case where the QD is coupled to a phonon reservoir at a temperature $T = 10$ K. The other parameters are as in Fig. 1.

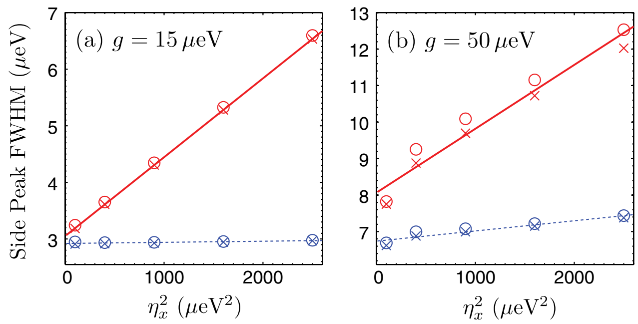

FIG. 4 (color online). FWHM of the Mollow sidebands (circles: low energy peak, crosses: high energy peak) as a function of η_x^2, extracted by a numerical fit from Fig. 3 in the presence of phonon coupling (red solid line) and with no phonon-coupling (blue dashed line). Solid and dashed curves show a linear fit.

two-photon truncation of the ME, and plot the dominant resonances with the blue circles and red crosses, respectively. We thus confirm that the two-photon enabled resonance near the original cavity mode is dominated by the second rung of the two-photon Jaynes-Cummings ladder states; remarkably, phonon coupling helps one to observe such resonances.

Finally, we make a direct connection to very recent experiments [15]. In Fig. 3 we show the cavity-emitted spectra of the QD exciton under resonant excitation conditions ($\Delta_{xL} = 0$) as a function of cw excitation Rabi frequency, for $g = 15\ \mu$eV and $g = 50\ \mu$eV. For clarity, we show spectra with and without phonon coupling, where, to be consistent with experiments [15], the former assumes a phonon reservoir in thermal equilibrium at $T = 10$ K. As expected, we find an increasing splitting of the Mollow triplet with increasing Rabi frequency η_x. We also note that the location of the sidebands changes due to the renormalization of the Rabi frequency in the presence of phonon coupling which reduces the effective Rabi frequency; the Mollow splitting is slightly reduced as a result and the triplet resonances are significantly broader. In Fig. 4, we plot the corresponding numerically extracted FWHM (full width half maximum) versus η_x^2. We also show a linear fit with η_x^2, which fits very well and agrees with the measurements [15]. However, for the case of $g = 50\ \mu$eV, the dependence is likely nonlinear for low values of η_x, and in general dephasing results from the interplay of both phonon bath coupling and cavity photon bath coupling. For increasing g, the lower energy triplet peak (circles) are broadened more than the high energy peak (cf. crosses) since it is nearer the cavity mode.

In summary, we have presented a theoretical and numerical study of the phonon-dressed, cavity-emitted resonance fluorescence of a QD placed inside a high-Q cavity. We developed a polaron ME formalism based on the time-convolutionless approach which enabled us to study the dynamical properties of the reduced density matrix of the QD-cavity system in response to both an external cw laser field and a bath of thermalized acoustic phonons. We applied this theory to study the influence of the Rabi frequency on cavity-emitted spectra and find strong numerical evidence of EID of the Mollow triplet and nonperturbative cavity feeding effects. Both multiphonon and multiphoton effects are highlighted, and our general findings are in good agreement with experiments [15].

This work was supported by NSERC. We gratefully acknowledge H. J. Carmichael for useful discussions, and S. M. Ulrich, S. Reitzenstein, and P. Michler for discussions and for sharing their experimental results [15]. We also acknowledge partial use of the quantum optics toolbox [27].

Note added.—After submission of our Letter, we became aware of related work on the off-resonant exciton cavity coupling [28].

*shughes@physics.queensu.ca

[1] S. Ates *et al.*, Phys. Rev. Lett. **103**, 167402 (2009).
[2] J. P. Reithmaier *et al.*, Nature (London) **432**, 197 (2004).
[3] T. Yoshie *et al.*, Nature (London) **432**, 200 (2004).
[4] D. Press *et al.*, Phys. Rev. Lett. **98**, 117402 (2007).
[5] A. Muller *et al.*, Phys. Rev. Lett. **99**, 187402 (2007).
[6] E. B. Flagg *et al.*, Nature Phys. **5**, 203 (2009).
[7] A. N. Vamivakas *et al.*, Nature Phys. **5**, 198 (2009).
[8] S. Ates *et al.*, Nat. Photon. **3**, 724 (2009).
[9] B. R. Mollow, Phys. Rev. **188**, 1969 (1969).
[10] See, e.g., H. J. Carmichael, *Statistical Methods in Quantum Optics 1* (Springer, New York, 1998).
[11] J. Förstner *et al.*, Phys. Rev. Lett. **91**, 127401 (2003).
[12] D. Mogilevtsev *et al.*, Phys. Rev. Lett. **100**, 017401 (2008).
[13] A. J. Ramsay *et al.*, Phys. Rev. Lett. **104**, 017402 (2010); A. J. Ramsay *et al.*, *ibid.***105**, 177402 (2010).
[14] A. Nazir, Phys. Rev. B **78**, 153309 (2008).
[15] S. M. Ulrich *et al.*, preceding Letter, Phys. Rev. Lett. **106**, 247402 (2011).
[16] G. D. Mahan, *Many-Particle Physics* (Plenum, New York, 1990), Section 4.3.
[17] I. Wilson-Rae and A. Imamoglŭ, Phys. Rev. B **65**, 235311 (2002).
[18] D. P. S. McCutcheon and A. Nazir, New J. Phys. **12**, 113042 (2010).
[19] Y. Ota *et al.*, arXiv:0908.0788.
[20] H. J. Carmichael and D. F. Walls, J. Phys. A **6**, 1552 (1973).
[21] F. Milde, A. Knorr, and S. Hughes, Phys. Rev. B **78**, 035330 (2008).
[22] S. Hughes *et al.*, Phys. Rev. B **83**, 165313 (2011).
[23] C. Roy and S. John, Phys. Rev. A **81**, 023817 (2010).
[24] B. Krummheuer, V. M. Axt, and T. Kuhn, Phys. Rev. B **65**, 195313 (2002).
[25] J. Xue *et al.*, J. Phys. Condens. Matter **20**, 325209 (2008).
[26] K. Hennessy *et al.*, Nature (London) **445**, 896 (2007); M. Kaniber *et al.*, Phys. Rev. B **77**, 161303(R) (2008); J. Suffczynski *et al.*, Phys. Rev. Lett. **103**, 027401 (2009); U. Hohenester *et al.*, Phys. Rev. B **80**, 201311 (2009).
[27] S. M. Tan, J. Opt. B **1**, 424 (1999).
[28] A. Majumdar *et al.*, arXiv:1012.3125v1.